Review of CALORRE Calorimeter Characterizations Under Laboratory and Irradiation Conditions

A. Volte, M. Carette, A. Lyoussi, G. Kohse, J. Rebaud, V. Valero, C. Reynard-Carette

Review of CALORRE Calorimeter characterizations under laboratory and irradiation conditions

A. Volte, M. Carette, A. Lyoussi, G. Kohse, C. Reynard-Carette

***Abstract*— This paper deals with the CALORRE differential calorimeter patented by Aix-Marseille University and the CEA in 2015. Firstly, the paper focuses on the presentation of the first prototype of CALORRE calorimeter qualified under real conditions during the MARIA irradiation campaign in 2015. Then, a review of the studies dedicated to different CALORRE calorimetric cells realized thanks to experimental characterizations under laboratory conditions is detailed. Several configurations were studied to determine the influence of the cell height, its horizontal fin geometry and the nature of the material of its structure on its response for a calibration protocol by generating a heat source inside each cell: linearity, sensitivity, range, reproducibility, response time and absolute temperatures. Finally, within the framework of a new research program called CALOR-I and financed by Aix-Marseille University foundation (A*Midex), an optimization of the calorimeter assembly and its design were carried out in order to remove contact thermal resistances and provide a new very compact CALORRE calorimeter suited for the in-core water loop of the MIT reactor (2 W.g^{-1}). The response of this new very compact calorimeter is estimated thanks to 3-D numerical thermal simulations under real conditions.**

***Index Terms*— Calorimeter, Nuclear Absorbed Dose Rate, On-line Measurements, Calibration, Irradiation campaign.**

I. Introduction

The high neutron and gamma fluxes as well as strong displacements per atom characterize conditions of material testing reactors (MTRs). These research reactors constitute major support research facilities and allow experimental and real-condition studies of the behaviour of fuels and inert materials (vessel, reflector, cladding, etc.) in an extreme radiation environment. These studies are important as they lead to progress on the understanding of the accelerated ageing of materials and/or of phenomena for advanced scenarios up to accidental conditions and consequently they bring data for safety issues, the life span of existing nuclear power plants and their advancements with new concepts. Therefore, new instrumentation is needed to measure online key parameters both before the experiments for the device design and during the experiments for the result interpretation.

The construction of the Jules Horowitz Reactor, a new MTR of 100 MWth nominal power with unequalled performances in Europe (high fast neutron flux of 5.5x10^{14} n/(cm².s) from 1 MeV leading to a high accelerated ageing up to 16 dpa/year and a high nuclear absorbed dose rate up to 20 W.g^{-1} in aluminum), initiated new collaborative research work [1, 2]. Since 2009 Aix-Marseille University and the CEA (within the framework of the joint laboratory LIMMEX - Laboratory for Instrumentation and Measurement in Extreme Environments) and its IN-CORE program - Instrumentation for Nuclear Radiations and Calorimetry online in REactor) have been developing a new research topic. More precisely, they have been focusing on innovation in instrumentation and advanced measurement methods for the quantification of key nuclear parameters such as neutron and photon fluxes and nuclear absorbed dose rate, also called nuclear heating rate. The online measurement of this latter quantity requires specific sensors: non-adiabatic calorimeters. With regard to the state of the art, two distinct sensors are used in MTRs: French differential calorimeters (CALMOS, CARMEN or CALORRE type) [3-8] or single-cell calorimeters (such as gamma thermometers or KAROLINA-type calorimeters) [9-15].

These two types of calorimeter allow the quantification of the nuclear absorbed dose rate thanks to temperature measurements and preliminary calibration under non-irradiation conditions from steady thermal states in the case of integrated heating elements or from transient thermal states in other cases. One main objective targeted for French differential calorimeters within the framework of the IN-CORE program (Instrumentation for Nuclear radiations and Calorimetry for online measurements inside research Reactor) and more recently of the new research program, called CALOR-I (compact-CALORimeter Irradiations inside the MIT research reactor) and funded by Aix-Marseille University foundation (A*Midex) and involving the Nuclear Reactor Laboratory of the MIT and the CEA (2020-2022), is the reduction of the sensor size with the CALORRE calorimeter.

The paper will present a review of recent work carried out on

This paper was submitted on October 1, 2021.
"The CALOR-I project leading to this publication has received funding from the Excellence Initiative of Aix-Marseille University - A*Midex, a French "Investissements d'Avenir" programme".
A. Volte, M. Carette, C. Reynard-Carette are with Aix Marseille Univ, Université de Toulon, CNRS, IM2NP, Marseille, France (e-mail: adrien.volte@univ-amu.fr, michel.carette@univ-amu.fr, christelle.carette@univ-amu.fr).
A. Lyoussi, is with CEA/DES/IRESNE/DER, Section of Experimental Physics, Safety Tests and Instrumentation, Cadarache, F-13108, Saint Paul-lez-Durance, France (e-mail: abdallah.lyoussi@cea.fr).
G. Kohse is with Massachusetts Institute of Technology, Nuclear Reactor Laboratory, Cambridge, Massachusetts, USA (e-mail: kohse@mit.edu).

this CALORRE calorimeter patented by AMU and the CEA in 2015. The experimental and numerical work allows the design and the characterization of several CALORRE configurations over a wide range of nuclear absorbed dose rate (up to 20 $W.g^{-1}$).

The first part of the paper will describe the first design of CALORRE calorimeter fabricated for a range up to 1 $W.g^{-1}$ and its first successful qualification under real conditions during an irradiation campaign inside the Polish MARIA reactor (in November 2015). The second part will be dedicated to the characterization of the response of 6 new configurations of CALORRE calorimetric cell by means of a comprehensive approach coupling experimental, theoretical and numerical work from laboratory conditions to nuclear environments. The experimental metrological characteristics of the 6 configurations, in terms of sensitivity, linearity, range, reproducibility and response time, will be detailed.

The last part will present new results obtained for a new very compact CALORRE calorimeter. This latter was designed within the framework of the CALOR-I program. It will be used for the mapping of the in-core water loop of the MIT reactor (MITR) in terms of nuclear absorbed dose rate. This kind of measurement by means of calorimeter was never realized inside this reactor. The criteria for the choice of this new very compact CALORRE calorimeter will be detailed (mass, size, temperature, sensitivity). Then, the numerical responses under real conditions of a new CALORRE differential calorimeter assembly will be presented for different external boundary conditions.

II. First CALORRE calorimeter prototype qualified under real conditions

MARIA is a pool type water and beryllium moderated reactor located in Poland at the National Center for Nuclear Research (Swierk). The fast and the thermal neutron fluxes are around $1.5x10^{14}$ $n.cm^{-2}.s^{-1}$ (NRJ) and $3.5x10^{14}$ $n.cm^{-2}.s^{-1}$ respectively leading to an expected nuclear heating rate up to 3 $W.g^{-1}$ for a thermal nominal power of 30 MW. The objective of the irradiation campaign inside the MARIA reactor was to qualify a first prototype of CALORRE (full-height) while mapping the H-IV A experimental channel. This channel is located into the last periphery of the reactor core. The thermal power of the reactor was fixed at 24 MW during this irradiation campaign [16].

A. The CALORRE calorimetric cell

The Fig. 1 shows schematics of the first type of CALORRE calorimetric cell which was developed and tested under real conditions during the irradiation campaign in the MARIA reactor. This configuration had the same head as that of CARMEN calorimetric cell in terms of geometry, height (equal to 23.1 mm [8]) and assembly with a heating element in order to compare the responses of these two sensor-designs under laboratory and/or real conditions.

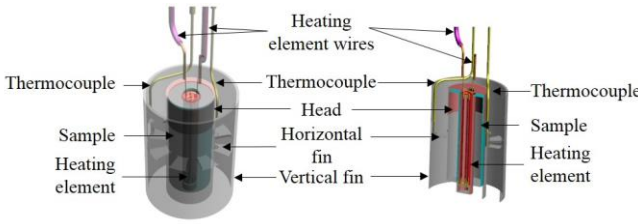

Fig. 1. A 3-D schemes of the first CALORRE calorimetric cell prototype (on the left-hand section) and of an internal view of this cell (on the right-hand section).

The heating element allows the simulation of the nuclear absorbed dose rate by Joule effect. The different parts of CALORRE calorimetric cell were already presented: a structure made of stainless steel AISI 316L which is composed of a head, a half horizontal-fin (8 metal sectors and 8 empty sectors with a same angle equal to 22.5 °) and a vertical fin , and an heating element with its holder, a sample in the case of the measurement cell and two K-type thermocouples to measure a temperature difference between two key points at hot and cold temperatures (T_{hot} and T_{cold}) respectively [5, 16-18]. This CALORRE calorimetric cell is called full-height and half horizontal-fin (cf. Fig. 1).

B. The CALORRE calorimeter

The CALORRE sensor is composed of two superimposed full-height and half horizontal-fin calorimetric cells. These identical cells host a graphite sample in the case of the measurement cell and gas (instead of the sample) for the reference cell. The reference cell is needed to remove the effect of the energy deposition on the structure of the measurement cell, the heating element, the heating element holder and the thermocouples.

The Fig. 2 gives a diagram of the complete CALORRE differential calorimeter. The two calorimetric cells are superimposed through the use of different thin spacers inside an external jacket and filled with di-nitrogen. This jacket is made of stainless steel (internal diameter equal to 17.0 mm and a thickness equal to 0.5 mm).

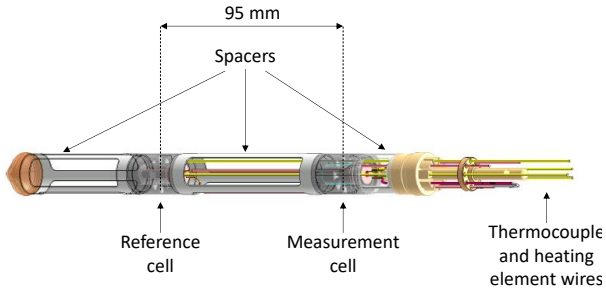

Fig. 2. 3-D scheme of the CALORRE differential calorimeter without its external additional jacket.

During the MARIA campaign, the distance between the two CALORRE cells was fixed to 71.9 mm leading to an inter-sample space of 95 mm (cf. Fig. 2). This important space was chosen in order to have the same distance than those used for previous common differential calorimeters (CALMOS or CARMEN).

C. Calibration of differential calorimeter under laboratory conditions and nuclear heating rate calculation

For each calorimetric cell (reference and/or measurement), a preliminary calibration step under laboratory conditions (without nuclear rays) is crucial to obtain its calibration curve. This kind of curve represents the difference of the mean steady temperatures between the two key points (T_{hot} -T_{cold}) versus the electrical power generated by the heating element integrated inside the cell head [16-18].

In the case of the first prototype of the CALORRE differential calorimeter, the two calorimetric cells were calibrated simultaneously. Thus, the calorimeter was inserted inside a Polish bench with a fluid flow vein at fixed temperature (40 °C) and velocity (corresponding to a Reynolds number equal to 17340) [16]. Then, different successive electrical current values were injected to each heating element in order to generate a power range from 0 to 6 W with an increment of 1 W in each calorimetric cell (cf. Fig. 3).

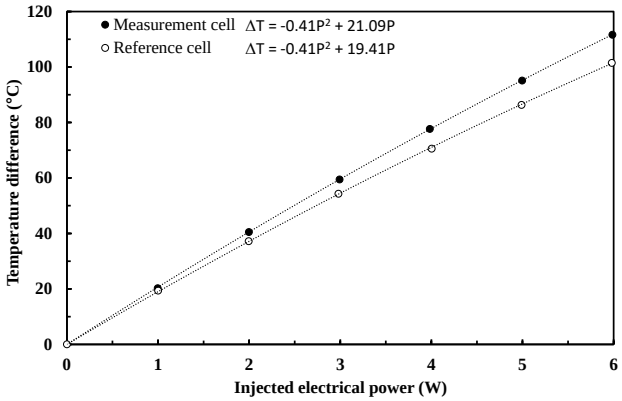

Fig. 3. Calibration curves of the superposed measurement and reference cells of the full-height and half horizontal-fin CALORRE configuration.

The responses of the two cells of the differential calorimeter are different leading to two different calibration curves:

$$(T_{hot} - T_{cold})_{measurement} = \Delta T_S = -0.42P^2 + 21.09P \quad (1)$$

$$(T_{hot} - T_{cold})_{reference} = \Delta T_R = -0.41P^2 + 19.41P \quad (2)$$

with P the electrical power injected in W.

These differences can be mainly due to mechanical defects such as the manufacturing of cell structure, the thermocouple position, the welding between each cell and the spacers but also due to the effects induced by the wires of the reference cell which passed through the horizontal-fin of the measurement cell.

Under real conditions inside the reactor, the nuclear heating rate (E_n) is determined by coupling these calibration curves with a heat balance by considering the weight of the sample, the heater, the sample-holder, the shim and the heater and a constant nuclear heating rate inside each calorimeter area.

Consequently, the response of each calorimeter cell is induced by the power deposited inside its head which is proportional to the nuclear heating rate. In the case of the measurement cell the deposited power P_S is given by:

$$P_S = P_{head} + P_{shim} + P_{sample-holder} + P_{heater} + P_{sample} = (m_1 + m_{sample})E_n \quad (3)$$

with m_1 the total mass corresponding to the head, shim, sample-holder, heater for the measurement cell, m_{sample} the sample mass.

In the case of the reference cell, the deposited power P_R becomes:

$$P_R = P_{head} + P_{shim} + P_{sample-holder} + P_{heater} = (m_2)\,E_n \quad (4)$$

with m_2 the total mass corresponding to the head, shim, sample-holder, heater for the reference cell masses respectively (head, shim, sample-holder, heater and wires).

By considering the formula from (1) to (4), the response of the differential calorimeter for the reference and the measurement cells located at the same axial position (z) inside the reactor can be given by:

$$\Delta T_S - \Delta T_R = A_{2S}\left((m_1 + m_{sample})\,E_n\right)^2 + A_{1S}(m_1 + m_{sample})\,E_n - A_{2R}\,(m_2 E_n)^2 - A_{1R}\,(m_2)\,E_n \quad (5)$$

with A_{1S} and A_{2S} the first-order and the second-order coefficients of the calibration curve of the measurement cell respectively; A_{1R} and A_{2R} the first-order and the second-order coefficients of the calibration curve of the reference cell respectively; ΔT_S and ΔT_R the in-pile steady temperature difference obtained for the measurement and reference cells respectively.

From this second-degree polynomial response, two solutions are possible but as the nuclear absorbed dose rate measured is upper than 0 W.g^{-1}, its value is deduced by:

$$E_n = \frac{-\left(A_{1S}(m_1+m_{sample}) - A_{1R}\,(m_2)\right) + \sqrt{\Delta}}{2\left(A_{2S}(m_1+m_{sample})^2 - A_{2R}\,(m_2)^2\right)} \quad (6)$$

with Δ the discriminant of the second-degree polynomial (5).

D. Operating protocol and MARIA irradiation campaign results

The calorimeter CALORRE was inserted into the experimental channel H-IV A thanks to a hollow cylindrical pipe (24.0 mm in internal diameter).

This jacket contained several holes in its lower part to allow the fluid flow around the sensors and linked in its upper part to a manual operated mechanical system used for the displacement of the device inside the channel. The device was moved by applying an axial increment equal to 95.0 mm (space induced by the position between the heads of the two superimposed calorimetric cells) from -463.0 mm to 487.0 mm (cf. Fig. 4) in order to obtain a mapping of the nuclear absorbed dose rate on ten axial positions. After each increment, around 20 minutes were waited to reach a steady state inside the calorimeter and to obtain the steady calorimeter response for more than 15 minutes.

As explained in section II.C, the nuclear absorbed dose rate at each axial position (z) is obtained by taking the two

calibration curves into account, and by measuring the mean steady temperature difference for the measurement cell located at the z-position (step i) and the mean steady temperature difference for the reference cell moved at the same z-position (step i+1).

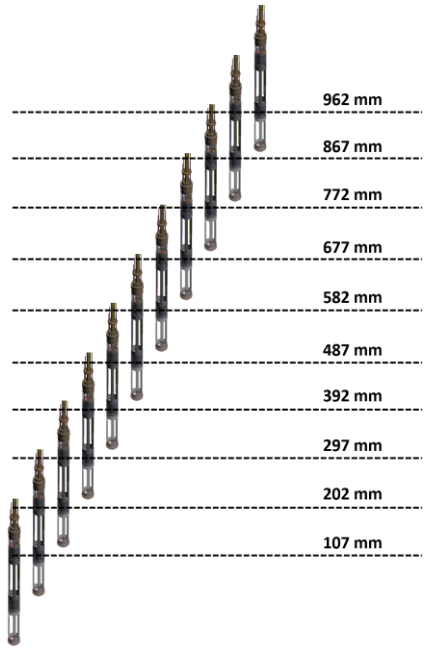

Fig. 4. Schematic of the operating protocol with the displacements for the 10 axial positions mapped inside the experimental channel.

The temporal responses of the two cells, obtained by following the previously defined operating protocol, are presented in the Fig. 5. The different steps and the steady-state regimes are visible for the temperature measurements of the two key points of each cell. The response time (average time needed for reaching 95 % of the final steady state value for each displacement) was about 290 s and 195 s for T_{hot} and T_{cold} of the measurement cell respectively as against 240 s and 180 s for T_{hot} and T_{cold} of the reference cell.

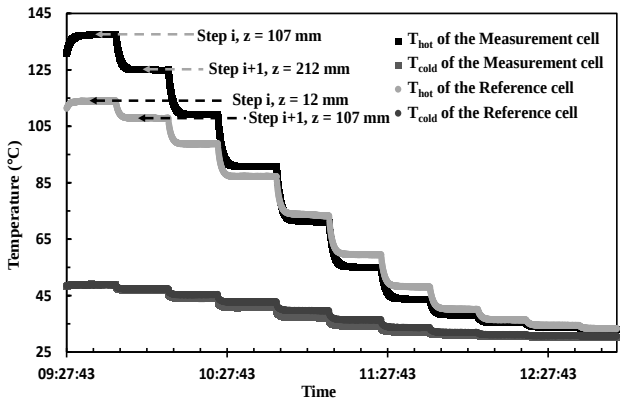

Fig. 5. Temporal responses of the two superposed cells of the CALORRE differential calorimeter during the mapping of the H-IV A experimental channel.

At the same position (z=107 mm), the hot temperature (T_{hot}) of the measurement cell is higher than that of the reference cell (137.7 °C as against 107.9 °C) due to the additional mass of the sample. The mean steady temperature differences (T_{hot} - T_{cold}) versus the axial position inside the experimental channel are deduced for the reference and the measurement cells for most of the axial positions specified in the operating protocol (cf. Fig. 6).

As expected, the temperature difference (T_{hot} - T_{cold}) is greater for the measurement cell, which is explained by the presence of the sample leading to a higher energy deposition.

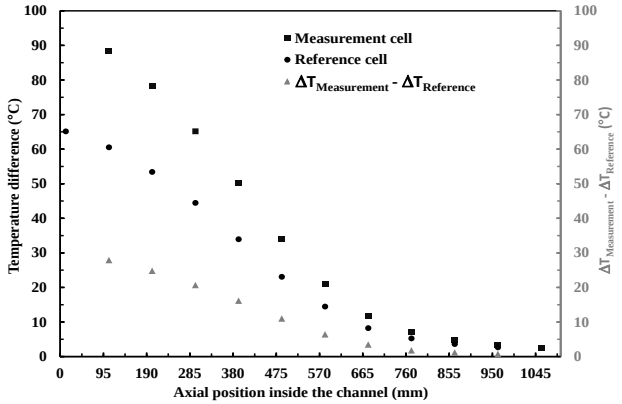

Fig. 6. Temperature differences versus the axial position inside the channel for the two superposed cells: measurement cell (y-axis on the left), reference cell (y-axis on the left) and ΔΔT (y-axis on the right).

As presented in section II.C, with the mean temperature difference versus the axial position inside the experimental channel H-IV A and of the calibration curve coefficients obtained under laboratory conditions, the nuclear absorbed dose rate can be calculated for each specific position (eq. 6). Finally, the axial profile of the H-IV A channel may be plotted.

The Fig. 7 shows the axial profile of the nuclear absorbed dose rate obtained with the first CALORRE calorimeter prototype having full-height and half horizontal-fin calorimetric cell configuration in stainless steel.

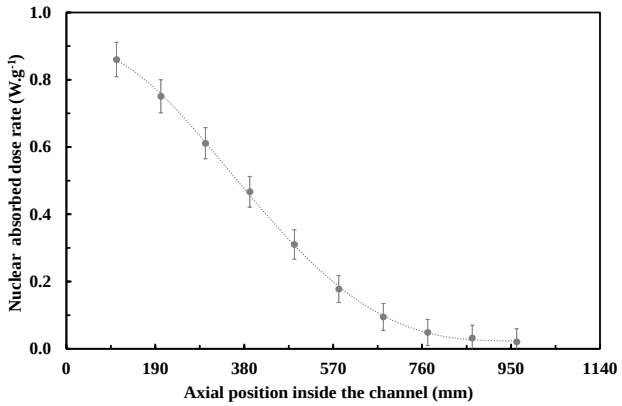

Fig. 7. Nuclear absorbed dose rate profile inside the H-IV A experimental channel of MARIA reactor measured by the first CALORRE calorimeter prototype.

In order to verify the proper functioning of the CALORRE-MARIA calorimeter, another in-pile measurement method, called zero-method [4, 8], was applied in two axial positions on the last day of the irradiation campaign (cf. Fig. 8). The difference with the previous measurement method is the adding

of a third step after the first two steps (which remained the same). In the third step, an electric current is injected into the heating element of the reference cell until the temperature difference of the reference cell is equal to that measured in step 1 for the measurement cell in the steady state. The nuclear absorbed dose rate is thus deduced directly from the electrical power injected into the reference cell, the mass of the measurement and reference cells (only the head structure, the wedge, the sample-holder and the heating element), the sample mass and the calibration coefficients for the sample and the reference cell. This method requires, as the first method, a preliminary calibration (under laboratory conditions) to determine the calibration coefficients of each cell.

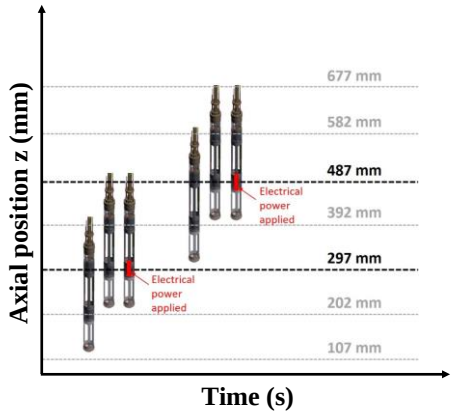

Fig. 8. Schematic of the operating protocol with the displacement and the different steps inside the experimental channel for the "zero method".

The results obtained with the two measurement methods show a slight deviation of 0 % and +3.3 % respectively at the +297 mm and +487 mm positions in the case of CALORRE-MARIA (cf. Table I).

TABLE I
RESULTS OF THE TWO METHODS (FIRST AND ZERO METHODS) APPLIED TO CALORRE-MARIA FOR TWO AXIAL POSITIONS

Axial position (mm)	297	487
$\Delta T_{measurement}$ without P_{elec} (°C)	64.9	33.0
$\Delta T_{reference}$ without P_{elec} (°C)	44.2	22.5
$\Delta\Delta T$ without P_{elec} (°C)	20.7	10.5
E_n with the first metho (W/g)	0.61	0.30
P_{elec} (W)	1.21	0.55
$\Delta T_{reference}$ with P_{elec} (°C)	64.6	32.4
$\Delta\Delta T$ with P_{elec} (°C)	0.3	0.5
E_n with the zero metho (W/g)	0.61	0.31

The ability to apply different measurement methods (including the current addition method, not presented in this paper) under real conditions is an advantage with this type of calorimeter owning a heating element and a reference cell. In conclusion, the first CALORRE calorimeter prototype was well behaved under real conditions. Consequently, a parametrical study on new configurations of calorimetric cell were performed in order to show the influence of different parameters, such as the structure material nature, the height of the cell and the horizontal-fin design, on the cell response. These results are presented in the next section.

III. PARAMETRICAL STUDY UNDER LABORATORY

In this section, the responses and metrological characteristics of 7 configurations of calorimetric cell (including that used during the MARIA irradiation campaign, called configuration N°1) are presented in Table II. Table II gives the height of the cell (H), the structure material nature (Material), the horizontal-fin geometry (Fin), the response time (t), the sensitivity at 6 W (S_{6W}), the total mass of the head structure (including shim, heating element and heating-element holder) and the sample (m), the absolute temperature located at the hot spot (T_{hot}) and the generated nuclear absorbed dose rate range (E_n) under laboratory conditions. They were obtained with the same set-up and operating protocol: only one calorimetric cell (the measurement cell) hosted by an external jacket [17-18] for same applied experimental conditions (T_{fluid}=33 °C and Re=1607) and with an electrical power range up to 6 W. The Fig. 9 presents the calibration curves of these 7 configurations.

First of all, the absolute temperature, the non-linearity and the sensitivity decreased with the increase of the number of metal sectors within the horizontal-fin geometry and with a higher thermal conductivity of the structure material.

Then, the change in the cell height (11.55 mm instead of 23.10 mm) did not impact significantly the sensitivity (in $°C.W^{-1}$) under laboratory conditions (16.2 $°C.W^{-1}$ for the configuration N°1 as against 15.1$°C.W^{-1}$ for the configuration N°6). In addition, the greater the height of the cell, the less resistive the gas layer is, thus increasing the conductive losses through the gas layer and so the non-linearity of the response. This is the first advantage of the reduced-height cell. The other advantage of the reduction of the cell height is the decreasing of the mass of the cell (~8 g for the configuration N°1 as against ~4.5 g for the configuration N°6) and so the mass of the sample (~1.4 g for the configuration N°1 as against ~0.6 g for the configuration N°6 for the graphite) which will induce lower absolute temperature under real conditions due to lower energy deposition and lower response time (291 s for the configuration N°1 as against 174 s for the configuration N°6). By against, the reduction in the sample mass will lead to a lower sensitivity (in $°C.g.W^{-1}$) under real conditions. Consequently, a reduced-height configuration is suited for higher values of nuclear heating rate compared to a full-height configuration.

This reduction in sensitivity under real conditions was confirmed by a validated predicted model based on a heat balance [19-20]. For example, the configuration N°1, had a sensitivity of 88.9 $°C.g.W^{-1}$ as against 49.6 $°C.g.W^{-1}$ for the

configuration N°6 (same characteristics except for its reduced height) at 1 $W.g^{-1}$.

TABLE II
METROLOGICAL CHARACTERISTICS FOR SEVEN CONFIGURATIONS OF A CALORRE CALORIMETRIC CELL

Configuration	N°1	N°2	N°3	N°4	N°5	N°6	N°7
H (mm)	23.1	23.1	23.1	23.1	23.1	11.55	11.55
Material (-)	AISI 316L	Al 5754	Al 5754	AISI 316L	AISI 316L	AISI 316L	TA6V
Fin (-)	1/2	1/4	1/2	1/4	1	1/2	1/4
t (s)	291	97	88	418	208	174	287
S_{6W} ($°C.W^{-1}$)	16.2	4.8	2.1	20.3	9.0	15.1	26.8
m (g)	5.22	3.20	3.20	5.22	5.22	2.92	2.16
T_{hot} (°C)	169	72	62	209	122	157	272
E_n ($W.g^{-1}$)	1.15	1.90	1.90	1.15	1.15	2.05	2.80

In addition, the aluminum configurations are suited to highest nuclear absorbed dose rate measurement [19-20] due to the low sensitivities.

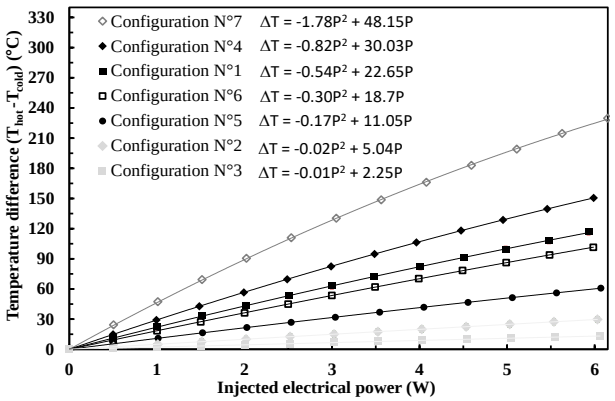

Fig. 9. Summary of calibration curves for 7 different CALORRE configurations.

More precisely, the full-height and half-surface aluminum configuration (configuration N°3) was qualified under laboratory conditions up to 60 W thanks to a new heating element system. This very large calibration range allowed the demonstration of the good running of the calorimetric cell for the maximal value of the nuclear absorbed dose rate inside the future JHR (20 $W.g^{-1}$) [19-20].

Finally, a last reduced-height configuration (N°7) was designed and tested in order to increase the sensor sensitivity compared to that of the configuration N°6. The titanium TA6V was chosen as structure material because it is less conductive than the stainless steel AISI 316L. In addition, the number of gas sectors was increased (12 as against 8) in order to increase the thermal resistance too. The mean calibration curve coefficients of this new configuration are equal to A_1=48.15 $°C.W^{-1}$ and A_2=-1.78 $°C.W^{-2}$. This configuration as expected corresponds to the most sensitive configuration but had the most non-linear response (cf. Fig. 9) as well as the highest absolute temperatures (272 °C) and a longer response time (287 s) than the reduced-height and half-surface configuration made of stainless steel (configuration N°6). By against, an advantage of this configuration N°7 is the reduction of the structure mass compared to those made of stainless steel due to the low density of the titanium TA6V (4500 $kg.m^{-3}$ against 7850 $kg.m^{-3}$) and consequently a less energy deposition in real conditions. Thus firstly, for the same level of nuclear absorbed dose rate under real conditions, the new compact calorimetric cell will be less subjected of the thermal radiative part and so can have a more linear response due to the lower absolute temperatures reached inside the calorimeter (reducing the radiative exchanges and the variation of thermal conductivity). Secondly, the electrical power range during the calibration step could be lower for a same level of nuclear absorbed dose rate. For instance, for an electrical power of 6 W injected inside the heating element of the configuration N°6, a nuclear absorbed dose rate of ~ 2.05 $W.g^{-1}$ is simulated during the calibration step as against ~ 2.80 $W.g^{-1}$ for the configuration N°7.

To conclude, on the one hand, this parametrical study under laboratory conditions showed a high modularity of the CALORRE calorimetric cells: sensitivity from 2.1 $°C.W^{-1}$ to 26.8 $°C.W^{-1}$ at 6 W leading to a wide measurement range. On the other hand, this study demonstrated the good behaviour of reduced-height calorimetric cells and the possibility to use them.

Consequently, with such reduced-height cells, the whole calorimeter could be less intrusive and more compact but also easier to couple with other sensors.

IV. NEW DESIGN OF A SPECIFIC MITR VERY COMPACT CALORRE CALORIMETER

This complete parametrical study was useful for the preparation of a new irradiation campaign which will be carried out within the framework of the new CALOR-I research program dedicated to the mapping of an in-core water-loop in the MIT reactor in term of nuclear absorbed dose rate. The core of the MIT reactor has a height of 56 cm and a diameter of 38 cm. The main maximal features are a thermal power of 6 MW, a thermal neutron flux of $3.6x10^{13}$ $n.cm^{-2}.s^{-1}$, a fast neutron (E > 1 MeV) flux of $1.2x10^{14}$ $n.cm^{-2}.s^{-1}$ and an expected nuclear absorbed dose rate of 2 $W.g^{-1}$ [21-22]. The temperature of the coolant fluid flow as well as its velocity can be changed inside the in-core water-loop. By considering the constraints of the experimental set-up used for the calibration under laboratory conditions [16-20] and located at AMU, the in-core water-loop fluid flow temperature will be fixed around 50 °C but the required speed of the fluid flow through the induced heat transfer coefficient will be studied to ensure energy evacuation.

A. The new CALORRE cell design

Regarding the previous irradiation campaign results, recent work [16-20], the results obtained for 6 other calorimetric cells and the expected nuclear absorbed dose rate inside the MITR, a very compact differential calorimeter with new reduced-height cells and a new assembly were defined and studied thanks to 3-D numerical thermal simulations with a COMSOL

Multiphysics finite element code coupled with a heat transfer module. The aims were to remove the thermal contact resistances by means of a simplification of each cell head and their assembly and to reduce the total height of the calorimeter.

As for a configuration with a reduced-height calorimetric cell (11.55 mm) and a half horizontal-fin design made of stainless steel, the experimental results under laboratory conditions and the predicted response under real conditions showed low absolute temperatures, low response time, a linear response and a good sensitivity, the configuration N°6 was chosen. But its vertical fin was increased in order to remove and replace the additional jacket which induced thermal contact resistances. Moreover, the sample and the head structure were made from a single block to avoid heater holders, other thermal contact resistances and to have the same material for the sample and the cell structure. Finally, the vertical fins of the measurement and the reference cells will be welded in order to eliminate the spacers (and thus additional energy deposition) and to obtain the whole calorimeter (cf. Fig. 10). An inter-cell space of 18 mm (leading to an inter-sample space of 29.55 mm) and a total height (excluding nose and cap) of 73.7 mm were defined. This new prototype corresponds to the smallest differential calorimeter ever designed. Its vertical size is similar to that of single-cell calorimeter.

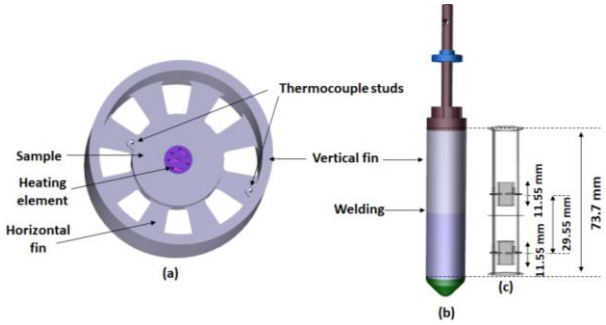

Fig. 10. Diagrams of the new CALORRE measurement calorimetric cell (a), the new assembly (b) and the geometry (c) considered for the 3-D numerical thermal simulations.

B. Study of the response under real conditions by 3-D numerical thermal simulations

The behaviour of this new compact differential calorimeter under real conditions (up to 2 W.g-1) was studied, by considering only the two cells (not the nose, the tail or the cables), thanks to the validated 3-D thermal model [20] integrating the following thermophysical properties (cf. Table III) and solved by using COMSOL Multiphysics for the steady state. The 3-D thermal model takes the thermal conductive transfers (thermal conductivity of stainless steel 316L and di-nitrogen as a function of temperature) and the thermal radiative transfers (constant emissivity of 0.2 for stainless steel 316L) into account. The global heat sources are determined from the expected nuclear absorbed dose rate range (up to 2 $W.g^{-1}$) and the density of the materials. Convective boundary limits are considered to the external surfaces of the calorimeter (turbulent fluid flow with a heat transfer coefficient (h) and a coolant fluid temperature (T_f)). A study of the influence of the heat transfer coefficient value on the sensor response, the maximal temperature and the wall temperature was carried out for a coolant fluid flow temperature equal to 50 °C.

TABLE III
THERMOPHYSICAL PROPERTIES OF THE MATERIALS COMPOSING THE CALORIMETRIC ASSEMBLY

Materials	Density ($kg.m^{-3}$)	Thermal conductivity ($W.K^{-1}.m^{-1}$)
Stainless steel 316L	7850	$4*10^{-6}*(T-273.15)*(T-273.15) + 0.013269*(T-273.15) + 13.534$ [23]
Alumina	3900	40
Di-nitrogen	1.185	$3.6969697*10^{-4}+9.74353924*10^{-5}*T-4.07587413*10^{-8}*T^2+7.68453768*10^{-12}*T^3$ [24]

The Fig. 11 shows the influence of the heat transfer coefficient on the maximal temperature for the highest value of nuclear heating rate expected in the MITR loop. The maximal temperature decreases from 388 °C to 311 °C when the heat transfer coefficient increases from 250 $W.°C^{-1}.m^{-2}$ to 12000 $W.°C^{-1}.m^{-2}$ respectively. This influence decreases significantly from 5000 $W.°C^{-1}.m^{-2}$. These values are well below the melting temperature of the stainless steel 316L (around 1400 °C).

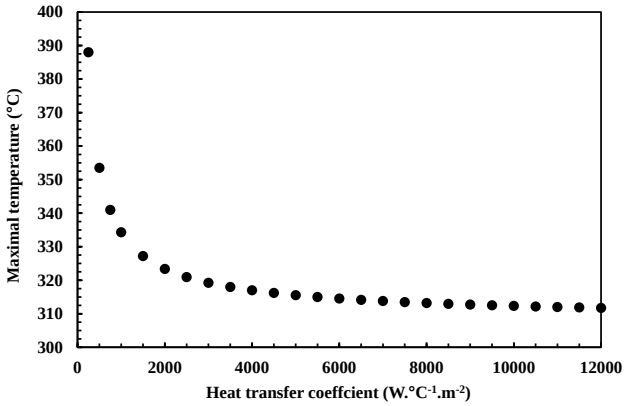

Fig. 11. Maximal temperature of the new very compact CALORRE calorimeter versus the external heat transfer coefficient and for a maximal nuclear absorbed dose rate equal to 2 $W.g^{-1}$ and a coolant fluid temperature of T_f=50 °C.

The same numerical study was analysed to observe the external temperature of the jacket from 5000 $W.°C^{-1}.m^{-2}$ to 12000 $W.°C^{-1}.m^{-2}$. In the same way as the maximum temperature, the wall temperature decreases as the coefficient h increases (cf. Fig. 12). The maximal wall temperature is lower than 60 °C for a heat transfer coefficient upper to 5000 $W.°C^{-1}.m^{-2}$ (56.1 °C and 55.3 °C for a heat transfer coefficient of 10000 and 12000 $W.°C^{-1}.m^{-2}$ respectively). This result demonstrates that there will be no wall boiling risk in the in-core water loop. Moreover, the temperature field (cf. Fig. 12) shows that there is no influence between the two cells, thus the inter-cell space is sufficient and does not require any additional specific study.

Finally, the response and the sensitivity of the new assembly were determined under real conditions for the same nuclear

heating rate range.

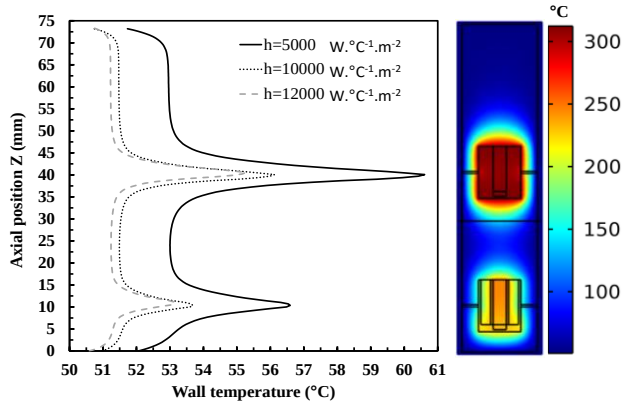

Fig. 12. Wall temperature of the new very compact CALORRE calorimeter versus the axial position (z) for three heat transfer coefficients (on the left-hand section) and the temperature field for h=10000 W.°C^{-1}.m^{-2} (on the right-hand section) for the maximal nuclear absorbed dose rate equal to 2 W.g^{-1} and a coolant fluid temperature T_f=50 °C.

The Fig. 13 shows the calculated responses of the measurement cell, the reference cell (on the left y-axis) and that of the calorimeter defined by the difference of the temperature differences (on the right y-axis) versus the nuclear absorbed dose rate for a heat transfer coefficient of 10000 W.°C^{-1}.m^{-2}.

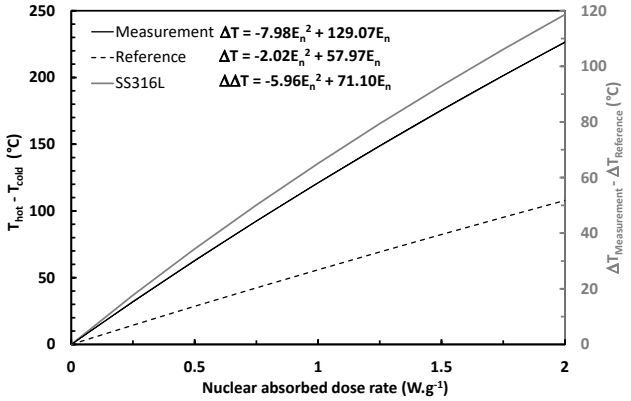

Fig. 13. 3-D numerical responses of the measurement cell (black line, left y-axis), the reference cell (black dashed line, left y-axis) and the whole calorimeter (grey line, right y-axis) versus the nuclear absorbed dose rate for the new very compact CALORRE calorimeter (h=10000 W.°C^{-1}.m^{-2} and T_f=50 °C).

Despite a non-linear response ($\Delta\Delta T$=-5.96E_n^2+71.10E_n) the sensitivity of the calorimeter is good for the whole range (47.26 °C.g.W^{-1} at 2 W.g^{-1}). The calorimeter can be used to quantify a nuclear absorbed dose rate from 0.08 W.g^{-1} considering the measurement uncertainties related to the thermocouples and the associated acquisition chain.

V. Conclusions

A first prototype of the new CALORRE differential calorimeter was fabricated and qualified successfully, by means of two measurement methods, under real conditions during an irradiation campaign inside the MARIA reactor in 2015. Moreover, this irradiation campaign allowed the validation of predictive and 3-D models under real conditions. Thereafter, 6 new configurations of a CALORRE calorimetric cell were fabricated and studied experimentally under laboratory conditions to show the influence of the structure material nature, the height of the cell and its horizontal-fin design on the cell response (linearity, sensitivity, response time, maximal temperature, …). One of these configurations suitable for JHR conditions (up to 20 W.g^{-1}) was qualified under laboratory conditions up to 60 W.

Finally, a new very compact design of CALORRE calorimeter for future experiments inside the MIT reactor was defined and studied under real conditions thanks to the validated 3-D thermal model. This new calorimeter prototype will have a reduced height never developed and similar to the axial space requirement of single-cell calorimeters. Moreover, the thermal contact resistances, previously observed, will be removed thanks to new cells without heating-element holders, a monobloc measurement cell with its sample and an assembly without spacers and without an additional jacket. A good behaviour and the influence of the heat transfer coefficient on the response and the maximal and wall temperatures were observed and determined numerically for this new calorimeter under real conditions. For instance, the maximal temperature, the wall temperatures and the sensitivity at 2 W.g^{-1} and for a heat transfer coefficient of 10000 W.°C^{-1}.m^{-2} are 312 °C, 56.1 °C and 47.26 °C.g.W^{-1} respectively.

Regarding the outlooks, numerical and experimental work will be done before the irradiation campaign. On the one hand the simulations of the interactions between radiations and matter with the MCNP Monte-Carlo transport code and nuclear data library will be realized in order to define the local heat sources in each part of the new calorimeter for MITR conditions. On the other hand, an experimental characterization of this new very compact sensor under laboratory conditions will be carried out.

Acknowledgment

"The CALOR-I project leading to this publication has received funding from the Excellence Initiative of Aix-Marseille University - A*Midex, a French “Investissements d’Avenir” programme”.

References

[1] A. Lyoussi, D. Fourmentel, J-F. Villard, J-Y. Malo, P.Guimbal, H. Carcreff, C. Gonnier, G. Bignan, J-P. Chauvin, C. Reynard-Carette, J. Brun, O. Merroun, M. Carette, M. Muraglia, A. Janulyte, Y. Zerega, J. Andre,"Advanced methodology and instrumentation for accurate on line measurements of neutron, photon and nuclear heating parameters inside Jules Horowitz MTR Reactor", Proceedings of Conferences RRFM and IGORR 2012, pp. 21-25, Prague, Czech Republic, 18-22 March 2012.

[2] G. Bignan, X. Bravo, P.M. Lemoine, "The Jules Horowitz Reactor: A new high Performances European MTR (Material Testing Reactor) with modern experimental capacities: Toward an International Centre of Excellence", Proceedings of Conferences RRFM and IGORR 2012, pp. 21-25, Prague, Czech Republic, 18-22 March 2012.

[3] C. Reynard-Carette, A. Lyoussi, J. Brun, M. Carette, M. Muraglia, A. Janulyte, Y. Zerega, J. André, G. Bignan, J-P. Chauvin, D. Fourmentel, C. Gonnier, P. Guimbal, J-Y. Malo, J-F. Villard, "Thermal study of a non adiabatic differential calorimeter used for nuclear heating measurements inside an experimental channel of the Jules Horowitz Reactor", Eurotherm 2012, Journal of Physics: Conference Series 395, pp. 1-9, 2012.

[4] H. Carcreff, V. Cloute-Cazalaa, and L. Salmon, “Development, calibration, and experimental results obtained with an innovative calorimeter (CALMOS) for nuclear heating measurements,” IEEE Trans. Nucl. Sci., vol. 59, no. 4, pp. 1369–1376, Aug. 2012.

[5] J. Brun, C. De Vita, C. Reynard-Carette, M. Carette, H. Amharrak, A. Volte and Abdallah Lyoussi, « Etude d'un nouveau capteur à transfert thermique radial mesurant l'énergie induite par interactions rayonnements nucléaires/matière, Acte du Congrès Français de Thermique (Toulouse, 31 mai - 3 juin 2016).

[6] C. De Vita, J. Brun, C. Reynard-Carette, M. Carette, H. Amharrak, A. Lyoussi, D. Fourmentel and J-F. Villard, “Study of the Influence of Heat Sources on the Out-of-Pile Calibration Curve of Calorimetric Cells Used for Nuclear Energy Deposition Quantification” IEEE Trans. Nucl. Sci., vol. 63, no. 4, pp. 2323–2330, Aug. 2016.

[7] C. Reynard-Carette, G. Kohse, J. Brun, M. Carette, A. Volte, A. Lyoussi, "Review of nuclear heating measurement by calorimetry in France and USA", Proc. ANIMMA 2017, Jun. 2017, EPJ Web of Conferences 170, 04019 (2018).

[8] H. Carcreff, L. Salmon and F. Malouch, “Recent developments in nuclear heating measurement methods inside the OSIRIS reactor”, Nucl. Instrum. Methods Phys. Res. A, Accel. Spectrom. Detect. Assoc. Equip., vol. 942, pp. 1-19, Oct. 2019.

[9] M. Tarchalski, K. Pytel, P. Siréta, A. Lyoussi, J. Jagielski, C. Reynard-Carette, C. Gonnier, G. Bignan, "Principle of calibration of the simple calorimeter for nuclear heating measurements in MARIA reactor and transposition to the case of JHR reactor", Proc. ANIMMA 2013, Jun. 2013.

[10] J. Brun, M. Tarchalski, C. Reynard-Carette, K. Pytel, A. Lyoussi, J. Jagielski, D. Fourmentel, J-F. Villard, M. Carette, "Responses of Single-Cell and Differential Calorimeters: From Out-of-Pile Calibration to Irradiation Campaigns," IEEE Trans. Nucl. Sci., vol.63, no. 3, pp. 1630 1639, Jun. 2016.

[11] A. Luks, K. Pytel, M.Tarchalski, N. Uzunow, T. Krok, “Modelling of thermal hydraulics in a KAROLINA calorimeter for its calibration methodology validation”, NUKLEONIKA, vol 61, no. 3, pp 453-460, Oct. 2016.

[12] M. S. Kim and B. G. Park, “Confirmation of Nuclear Heating Rate for Installation of Cold Neutron Source at HANARO”, in Proc. ANIMMA, Jun. 2019, EPJ Web of Conferences 225, 04004 (2020).

[13] R. Van Nieuwenhove, L. Vermeeren, “Nuclear heating measurements by gamma and neutron thermometers”, in Proc. ANIMMA, Jun. 2019, EPJ Web of Conferences 225, 04003 (2020).

[14] Rohanda, A., Waris, A., Kurniadi, R. *et al.* Validation and improvement of gamma heating calculation methods for the G.A. Siwabessy multipurpose reactor. *NUCL SCI TECH* **31,** 112 (2020).

[15] M. Alqahtani, A. Buijs, and S.E. Day, “Experimental measurement and Monte Carlo code simulation of the gamma heating at different irradiation sites in a nuclear research reactor”, Nucl. Eng. Des., 364 (2020), Article 110690.

[16] Julie Brun, Adrien Volte, Christelle Reynard-Carette, Michel Carette, Abdallah Lyoussi, Damien Fourmentel, Loïc Barbot, Jean-François Villard and Philippe Guimbal, “Nouveau capteur compact pour la mesure de l'échauffement nucléaire : Conception par simulation, Etudes en laboratoire, Qualification en réacteur de recherche”, Acte du Congrès Français de Thermique (Marseille, 30 mai - 2 juin 2017).

[17] A. Volte, C. Reynard-Carette, J. Brun, C. De Vita, M. Carette, T. Fiorido, A. Lyoussi, D. Fourmentel, J-F. Villard and P. Guimbal, " Study of the Flow Temperature and Ring Design Influence on the Response of a New Reduced-Size Calorimetric Cell for Nuclear Heating Quantification", Proc. ANIMMA 2017, Jun. 2017, EPJ Web of Conferences 170, 04026 (2018).

[18] A. Volte, C. Reynard-Carette, A. Lyoussi, J. Brun, M. Carette, "Study of the Response of a New Compact Calorimetric Cell for Nuclear Heating Rate Measurements", IEEE Trans. Nucl. Sci., vol. 65, no. 9, pp. 2461-2470, Sept. 2018.

[19] A. Volte, C. Reynard-Carette, A. Lyoussi, J. Brun, M. Carette, " Comparison of the Responses of New Reduced-Size Calorimetric Cells Made of Different Structure Materials for High Energy Deposition ", Proc. ANIMMA 2019, Jun. 2019, EPJ Web of Conferences 225, 04008 (2020).

[20] A. Volte, J. Brun, A. Lyoussi, M. Carette, C. Reynard-Carette, “Qualification of a New Differential Calorimeter Configuration Dedicated to Nuclear Heating Rates up to 20 W.g-1”, IEEE Trans. Nucl. Sci., vol. 67, no. 11, pp. 2405-2414, Nov. 2020.

[21] S. Kim, D. Carpenter, G. Kohse, L. Hu “Hydride fuel irradiation in MITR-II: Thermal design and validation results”, Nucl. Eng. Des., 277 (2014), pp. 1-14.

[22] A. J. Dave, K. Sun, L. Hu, E. Wilson, S. Pham, D. Jaluvka, “Thermal-hydraulic analyses of MIT Reactor LEU Transition Cycles,” Progress in Nuclear Energy 118 (2020):103-117.

[23] L. Kowalski, J. Duszczyk, L.Katgerman “Thermal conductivity of metal powder-polymer feedstock for powder injection moulding”, Journal of Materials Science, vol. 34, pp. 1-5, Jan 1999.

[24] COMSOL Multiphysics® v. 5.6. www.comsol.com. COMSOL AB, Stockholm, Sweden.